Paper presented at the Nat. Conf. on Few-Body and Quark-Hadronic Systems, Kharkov, Ukraine, June 1–5 TRI–PP–92–47 June 1992

ETA PHOTOPRODUCTION ON NUCLEONS AND LIGHT NUCLEI §

L. Tiator[1], *S.S. Kamalov*[1,2] *and C. Bennhold*[3]

[1] Institut für Kernphysik, Universität Mainz, D–6500 Mainz, Germany
[2] Laboratory of Theoretical Physics, JINR Dubna, Russia
[3]TRIUMF, 4004 Wesbrook Mall, Vancouver, B.C., V6T 2A3, Canada

Abstract

Eta photoproduction on the nucleon is studied in a model containing baryon resonances, nucleon Born terms and t-channel vector meson exchange and is compared to existing data. In nuclear application we present differential cross sections for d, ^{3}He, ^{3}H and ^{4}He. In particular photoproduction on the deuteron and ^{3}He will be ideal in order to study the elementary reaction on the neutron and subsequently the isoscalar excitation of the $S_{11}(1535)$ resonance.

1. Introduction

During the last few years, there have been a number of theoretical advances and experimental developments in the field of electron scattering and the structure of baryons and mesons. With the advent of high duty cycle electron accelerators very precise data has been obtained, e.g. for threshold π^0 photoproduction on the proton. The unexpected deviation between these results and theoretical predictions mainly based on the low energy theorems (*LET*) triggered a series of theoretical activities in the field of meson photoproduction[1]). With the recent completion of the modern electron accelerators at Mainz and Bonn and the construction of new detectors it is now possible to measure eta photoproduction from threshold at 709 MeV up to 850 MeV at Mainz and even higher energies at Bonn with a similar precision as pion photoproduction. A large amount of data has already been taken and is currently being analysed[2,3]). These upcoming results will improve our knowledge of the (γ,η) process enormously; currently it is only based on some very old measurements of 20 years ago[4,5]) and some more recent data from Tokyo[6]) and Bates[7]).

Unlike pion photoproduction, no *LET* can be derived for eta photoproduction for 3 good reasons: (*i*) The expansion parameter $\mu = m_\eta/m_N \approx 0.6$ is too large to provide convergence up to order μ^2; (*ii*) due to large $\eta-\eta'$ mixing with a mixing angle of about 20° and a non-conserved axial singlet current A_0^μ for the η', there is no *PCAC* theorem for eta mesons; (*iii*) there are nucleon resonances, mainly the $S_{11}(1535)$ close at threshold ($W_{thr.} = 1478$ MeV) violating strongly the condition that the internal excitation energy must be larger than the mass of the meson.

Therefore it is not surprising that nucleon resonance excitation is the dominant reaction process in (γ,η). Firstly in contrast to pions which will excite $\Delta(T=3/2)$ as well as $N^*(T=1/2)$ resonances, the η meson will only appear in the decay of N^* resonances with $T=1/2$. In the low-energy region this is dominantly the $S_{11}(1535)$ state that decays in 45-55% into ηN, the only nucleon resonance with such a strong branching ratio in the η channel. This result is even more surprising as a near-by resonance of similar structure, the $S_{11}(1650)$ has a branching ratio of only 1.5%. This "η puzzle" is not yet understood in quark models of the nucleon.

The first attempt to describe (γ,η) on the nucleon was made in 1973 by Hicks et al[8]) who fitted a series of nucleon resonance parameters to the available data. This model was improved by Tabakin at al[9]) in 1989. Benmerrouche and Mukhopadhyay used a lagrangian method and added to the nucleon resonances the nucleon Born terms and vector meson exchange contributions[10]).

§This work was supported by the Deutsche Forschungsgemeinschaft (SFB201) and the National Science and Engineering Research Council of Canada (NSERC).

In a very different approach, Bennhold and Tanabe[11]) derived a dynamical model which employs $\pi N \to \pi N, \pi N \to \pi\pi N$ and $\pi^- p \to \eta n$ to fix the hadronic vertex as well as the propagators and the $\gamma N \to \pi N$ to construct the electromagnetic vertex. In this way this method is more a prediction than a fit for the $\gamma N \to \eta N$ reaction.

The aim of our paper is to extend the model of Bennhold and Tanabe by taking into account the background from s,u-channel nucleon Born terms and ρ,ω exchange in the t-channel and to apply the operator on elastic eta photoproduction reactions on the lightest nuclei, d, ^{3}He, ^{3}H and ^{4}He. Due to spin and isospin selection rules, a combination of all these light nuclei with well-known nuclear structure will finally allow us a complete determination of the individual multipoles of (γ,η) for protons and neutrons as well. For instance, a very elementary question concerning the structure of the S_{11} resonance and the "η puzzle" will be: "How large is the isoscalar amplitude?".

In section 2 we will shortly summarize the resonance model of Bennhold and Tanabe and will describe our full (γ,η) operator. This will be compared to the existing data on the proton. The formalism of (γ,η) on nuclei will be derived in a coupled channel framework with complete final state interaction in section 3 and predictions for differential cross sections of elastic (γ,η) on d, ^{3}He, ^{3}H and ^{4}He will be given. In section 4 we will summarize our results and give some conclusions.

2. Eta photoproduction on the nucleon

The dynamical model of Bennhold and Tanabe[11]) is based on the observation that near η production threshold three nucleon resonances $P_{11}(1440)$, $D_{13}(1520)$ and $S_{11}(1535)$ play an important role. Assuming an isobar model for each partial wave the transition amplitude can be written as

$$t_{ij}(W) = f_i^\dagger D^{-1}(W) f_j \tag{1}$$

where W is the invariant energy and $i,j = \pi,\eta$ denotes the πN and ηN channels, respectively. The vertex functions f_i are parametrized with coupling strengths and formfactors and the N^* propagators are given by

$$D(W) = W - m_0 - \Sigma_\pi(W) - \Sigma_\eta(W) + \frac{i}{2}\Gamma_{\pi\pi}(W) \tag{2}$$

with the bare resonance mass m_0.

The self-energy Σ associated with the πN and ηN intermediate states is given by

$$\Sigma_i(W) = \int_0^\infty \frac{q^2 dq}{(2\pi)^3} \frac{M}{2w_i(q)E_N(q)} \left(\frac{q}{m_i}\right)^{2l} \frac{g_i^2(1+q^2/\Lambda_i^2)^{-2-l}}{W - w_i(q) - E_N(q) + i\epsilon} \tag{3}$$

with $w_i(q) = \sqrt{m_i^2+q^2}$, $E_N(q) = \sqrt{M^2+q^2}$ and M denoting the nucleon mass. The 2π–decay width $\Gamma_{\pi\pi}$ is parametrized with one free parameter. The six parameters in this approach have been determined for each partial wave by a least-squares fit to all data of the reactions $\pi N \to \pi N$, $\pi N \to \pi\pi N$ and $\pi^- p \to \eta n$ and can be found in ref.[11])

For a convenient use of this operator, especially in nuclear application with multidimensional integrals, we have obtained simple parametrizations of the self-energy Σ, eq. (3), in very good agreement with the exact numerical values.

$$Re\,\Sigma = a + (b_1\sqrt{x} + b_2 x^2)\Theta(-x) + (c_1 x + c_2 x^2)\Theta(x)\,, \tag{4a}$$

$$Im\,\Sigma = (d_1\sqrt{x} + d_2 x + d_3 x^2)\Theta(x) \tag{4b}$$

with $x = (W - M - m_i)/m_\pi$, $i = \pi,\eta$ and the step function $\Theta(x)$. The parameters are given in table 1. Finally the decay width in the 2π–channel is given by

		a	b_1	b_2	c_1	c_2	d_1	d_2	d_3
S_{11}	πN	17	0	0	0	0	-129.5	80	-5
	ηN	-27	17.7	-1.23	22.9	-5.17	-38.1	18.3	0
P_{11}	πN	-150	0	0	0	0	55.1	-96.2	6.6
D_{13}	πN	-26	0	0	0	0	23	-32.1	2.7

Table 1: Parameters for the πN and ηN self-energies in MeV

$$\Gamma_{\pi\pi}(W) = \gamma x \Theta(x), \qquad x = (W - M - 2m_\pi)/m_\pi \tag{5}$$

with $\gamma(S_{11}) = -18.3MeV$, $\gamma(P_{11}) = 80.3MeV$ and $\gamma(D_{13}) = 24.2MeV$.

With the hadronic vertex and propagators being determined, the photoproduction amplitudes for (γ,π) and (γ,η) are given by

$$t_{i\gamma}(W) = V^B_{i\gamma}(W) + f_i^\dagger D^{-1}(W)\tilde{f}_\gamma , \tag{6}$$

where $V^B_{i\gamma}$ are the Born terms and $\tilde{f}_\gamma$ the electromagnetic vertex. The latter was determined by using the pion photoproduction data. In this way there are no free parameters left for the (γ,η) process which will turn out as a prediction rather than a fit in this model. Since in ref.[11]) the Born terms in the η-channel have been neglected, $V^B_{\eta\gamma} \equiv 0$, this model consists out of four (γ,η) multipoles only: From $S_{11}(1535)$ the strongly dominating E_{0+}, from $P_{11}(1440)$ the M_{1-} and from $D_{13}(1520)$ the E_{2-} and M_{2-}.

Whereas the neglect of the (γ,η) Born terms are within the uncertainties of the older experimental data for the proton, they can play a more important role when better data will become available and will become absolutely necessary in nuclear reactions like the coherent η photoproduction on ^{4}He, where the dominant excitation of the S_{11} resonance is forbidden. The evaluation of the background terms is straightforward and in complete analogy to (γ,π^0) except to the fact that the η is an isoscalar meson. Furthermore the pseudoscalar coupling of the ηN is not ruled out by LET as in the case of (γ,π), in fact, as we will show later, present experimental data are in favour of the PS instead of the PV coupling.

The effective lagrangians for ηN coupling are given by

$$\mathcal{L}^{PS}_{\eta NN} = -ig_\eta \bar{\psi}\gamma_5\psi\phi_\eta , \qquad \mathcal{L}^{PV}_{\eta NN} = \frac{g_\eta}{2M}\bar{\psi}\gamma_\mu\gamma_5\psi\partial^\mu\phi_\eta . \tag{7}$$

With the electromagnetic lagrangian

$$\mathcal{L}^{PS}_{\gamma NN} = -ie\bar{\psi}\gamma_\mu\frac{1+\tau_0}{2}\psi A^\mu + \frac{e}{4M}\bar{\psi}(\kappa^S + \kappa^V\tau_0)\sigma_{\mu\nu}\psi F^{\mu\nu} , \tag{8}$$

where $\kappa^S = -0.06$ and $\kappa^V = 1.85$ are the isoscalar and isovector anomalous magnetic moments and $F^{\mu\nu} = \partial^\nu A^\mu - \partial^\mu A^\nu$ we can evaluate the s- and u-channel Born terms. Expressed in the $CGLN$ basis

$$F = iF_1\vec{\sigma}\cdot\vec{\epsilon} + F_2\vec{\sigma}\cdot\hat{\vec{q}}\sigma\cdot(\hat{\vec{k}}\times\vec{\epsilon}) + iF_3\vec{\sigma}\cdot\hat{\vec{k}}\hat{\vec{q}}\cdot\vec{\epsilon} + iF_4\vec{\sigma}\cdot\hat{\vec{q}}\hat{\vec{q}}\cdot\vec{\epsilon} \tag{9}$$

we obtain the following amplitudes for pseudoscalar coupling

$$F_1(PS) = g_\eta C\left[\left(-e_N + \frac{W-M}{2M}\kappa_N\right)D + \frac{(t-m_\eta^2)\kappa_N}{2M(W-M)(u-M^2)}\right] , \tag{10a}$$

$$F_2(PS) = g_\eta \frac{C\,|\vec{q}\,|}{E_2+M}\left[\left(e_N + \frac{W+M}{2M}\kappa_N\right)D + \frac{(t-m_\eta^2)\kappa_N}{2M(W+M)(u-M^2)}\right] , \tag{10b}$$

$$F_3(PS) = g_\eta C\,|\vec{q}\,|\left[2e_N\frac{W-M}{t-m_\eta^2}D - \frac{\kappa_N}{M(u-M^2)}\right] , \tag{10c}$$

$$F_4(PS) = g_\eta \frac{C\,|\vec{q}\,|^2}{E_2+M^2}\left[-2e_N\frac{W+M}{t-m_\eta^2}D - \frac{\kappa_N}{M(u-M^2)}\right] , \tag{10d}$$

where $t = 2(\vec{k}\cdot\vec{q} - E_\gamma E_\pi) + m_\eta^2$, $u = -2(\vec{k}\cdot\vec{q} + E_\gamma E_2) + M^2$, $E_{1(2)}$ is the nucleon energy in the initial (final) state, and

$$C = -e\frac{W-M}{8\pi W}\sqrt{(E_1+M)(E_2+M)} , \qquad D = \frac{1}{W^2-M^2} + \frac{1}{u-M^2} . \tag{11}$$

For pseudovector coupling we get

$$F_1(PV) = F_1(PS) - g_\eta\frac{C\kappa_N}{2M^2}, \qquad F_2(PV) = F_2(PS) + g_\eta\frac{C\,|\vec{q}\,|\,\kappa_N}{2M^2(E_2+M)}, \tag{12}$$

and no change for $F_{3,4}$.

In the above equations (where $N = p,n$) the amplitudes are expressed for the protons and neutrons separately with $e_p = 1$, $e_n = 0$ and $\kappa_p = 1.79$, $\kappa_n = -1.91$. Alternatively we can define the isoscalar and isovector amplitudes $F_i^{(0)}$ and $F_i^{(1)}$ by

$$F_i = F_i^{(0)} + F_i^{(1)}\tau_0 \tag{13}$$

Due to the decay of the vector mesons $V(J^\pi;T) = \omega(1^-;0)$ and $\rho(1^-;1)$ into $\eta\gamma$ we also have to include the t-channel Born diagrams which we evaluate from the lagrangians

$$\mathcal{L}_{VNN} = -g_V\bar{\psi}\gamma_\mu\psi V^\mu + \frac{g_T}{4M}\bar{\psi}\sigma_{\mu\nu}\psi V^{\mu\nu} , \qquad \mathcal{L}_{V\eta\gamma} = \frac{e\lambda_V}{4m_\eta}\varepsilon_{\mu\nu\lambda\sigma}F^{\mu\nu}V^{\lambda\sigma}\phi_\eta \tag{14}$$

with $V^{\mu\nu} = \partial^\nu V^\mu - \partial^\mu V^\nu$ like the e.m. field tensor $F^{\mu\nu}$. This yields to the $CGLN$ amplitudes

$$F_1(V) = \frac{\lambda_V C}{m_\eta(t-m_V^2)}\left[-\frac{g_T}{2M}t + \left(\frac{t-m_\eta^2}{2W-2M} + W - M\right)g_V\right] , \tag{15a}$$

$$F_2(V) = \frac{\lambda_V C}{m_\eta(t-m_V^2)}\frac{|\vec{q}\,|}{E_2+M}\left[\frac{g_T}{2M}t + \left(\frac{t-m_\eta^2}{2W+2M} + W + M\right)g_V\right] , \tag{15b}$$

$$F_3(V) = \frac{\lambda_V C}{m_\eta(t-m_V^2)}\,|\vec{q}\,|\left[\frac{g_T}{2M}(W-M) - g_V\right] , \tag{15c}$$

$$F_4(V) = -\frac{\lambda_V C}{m_\eta(t-m_V^2)}\frac{|\vec{q}\,|^2}{E_2+M}\left[\frac{g_T}{2M}(W+M) + g_V\right] . \tag{15d}$$

Due to the isospin, the ω contributes only to $F_i^{(0)}$ and ρ only to $F_i^{(1)}$.

In table 2 we give the coupling constants and cut-off masses for the background contributions. For the vector mesons we have introduced dipole formfactors $F(\vec{k}^2) = (\Lambda_V^2 - m_V^2)^2/(\Lambda_V^2 + \vec{k}^2)^2$ on the VNN vertex given by the Bonn potential, for the ηNN coupling the formfactors turned out to be insensitive and have been ignored. The c.m. $V\eta\gamma$ couplings are obtained from the partial decay

V	g_V	g_T	Λ_V	λ_V
ω	17	0	1.4 GeV	0.192
ρ	2.5	15.25	1.8 GeV	0.89

Table 2: Coupling constants and cut–off masses for the background vector meson exchange contributions. For the Born s– and u–channels we used $g_\eta^2/4\pi$=1.4.

widths of the vector mesons. The largest uncertainty, however, appear in the ηNN coupling. Here not even the structure of the coupling PS or PV is known. For the coupling constant $g_\eta^2/4\pi$ the values in the literature range between 1 and 5, the larger ones are found in the Bonn potential[12]) while the smaller values are preferred by the current (γ,η) data on the proton. An important aim of the eta photoproduction will also be a better determination on this coupling constant which is rather insensitive in NN interaction.

target	$S_{11}(1535)$	Born PS	Born PV	$\omega+\rho$
proton	13.1	-6.2	-1.1	3.0
neutron	-7.2	4.2	-1.2	-2.3

Table 3: Contributions to the threshold amplitudes of ReE_{0+} in units of $10^{-3}/m_\pi$

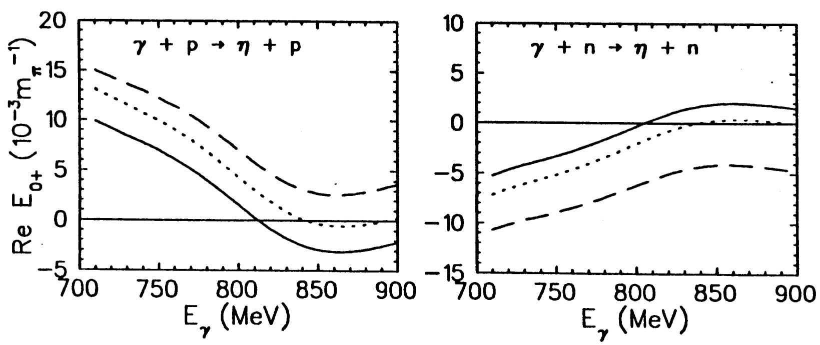

Fig. 1: Real part of the E_{0+} amplitude for (γ,η) on proton and neutron. The dotted line gives the pure resonance model from ref.[11]) and the dashed and full lines show the inclusion of PV and PS background terms respectively.

In table 3 we give the individual contributions for the real part of the threshold amplitude E_{0+} for protons and neutrons and in Fig. 1 we show the energy dependence up to $900MeV$. Both multipoles are dominated by the $S_{11}(1535)$ dipole resonance. Similar as in quark model calculations, also in the Bennhold–Tanabe approach it turns out to be mainly isovector with $E_{0+}^{(0)}/E_{0+}^{(1)} = 0.29$ for the resonance. Taking into account the background contribution this result

changes only slightly for PS (0.31) and gets even smaller for PV coupling (0.17). Whereas the PV coupling gives an enhancement of the E_{0+} multipole, the PS coupling reduces the amplitude. The same signature appears in the total cross section of Fig. 2, where we compare our results with the existing data. From these results a clear preference to either coupling is not possible. This changes, however, in the case of the differential cross sections in Fig. 3. The PV coupling clearly overestimates the data and the PS model is experimentally preferred. Both figures demonstrate the need for new and precise experimental data that is already in the analysis[2,3]).

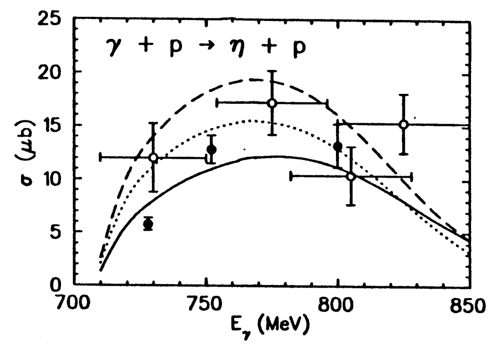

Fig. 2: Total cross section for $\gamma p \to \eta p$ near threshold. The curves are as in Fig. 1, the experimental data are from ref. [7]) (•) and ref. [13]) (o).

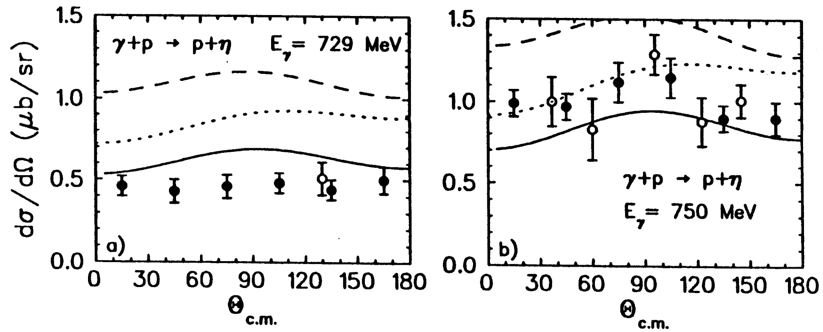

Fig. 3: Differential cross section for $\gamma p \to \eta p$ at E_γ = 729 MeV (a) and 750 MeV (b). The curves are as in Fig. 1. The experimental data are from ref. [7]) (•) and ref. [4]) (o).

3. Eta photoproduction on nuclei

Eta photoproduction on nuclei can be developed in a straightforward way by the same method which has been applied very successfully in pion photoproduction[14]). In momentum space the nuclear photoproduction amplitude can be written as

$$F_{\eta\gamma}(\vec{q},\vec{k}) = V_{\eta\gamma}(\vec{q},\vec{k}) - \frac{a}{(2\pi)^2}\sum_{i=\pi,\eta}\int \frac{d^3q'}{M_i(q')}\frac{F_{\eta i}(\vec{q},\vec{q}\,')\,V_{i\gamma}(\vec{q}\,',\vec{k})}{\mathcal{E}_\eta(q)-\mathcal{E}_i(q')+i\epsilon}\,, \qquad (16)$$

where $\vec{k}$ is the photon, and $\vec{q}$ is the eta or pion momentum. The total energy in the η-nucleus and π-nucleus channels is denoted by $\mathcal{E}_i(q) = E_i(q) + E_A(q)$, the reduced mass is given by $M_i(q) = E_i(q)E_A(q)/\mathcal{E}_i(q)$ and $a = (A-1)/A$.

$V_{\eta\gamma}$ is expressed in terms of the free eta–nucleon photoproduction t–matrix

$$V_{\eta\gamma}(\vec{q},\vec{k}) = -\frac{\sqrt{M_\eta(q)M_\gamma(k)}}{2\pi} < \eta(\vec{q}), n \mid \sum_{j=1}^{A} t_{\gamma N}(j) \mid 0, \gamma(\vec{k}) >, \qquad (17)$$

where $\mid n >$ and $\mid 0 >$ denote the nuclear initial and final states, respectively, and j refers to the individual target nucleons.

Using the KMT version of multiple scattering theory[15]) the meson scattering amplitude $F_{\eta i}$ is constructed as a solution of the Lippmann-Schwinger equation

$$F_{ij}(\vec{q}',\vec{q}) = V_{ij}(\vec{q}',\vec{q}) - \frac{a}{(2\pi)^2} \sum_{l=\pi,\eta} \int \frac{d^3q''}{M_l(q'')} \frac{V_{il}(\vec{q}',\vec{q}'')\, F_{lj}(\vec{q}'',\vec{q})}{\mathcal{E}_j(q) - \mathcal{E}_l(q') + i\epsilon}\,, \qquad (18)$$

Here the meson-nuclear interaction is described by the first-oder potential $V_{ij} = (V_{\pi\pi}, V_{\eta\pi}, V_{\eta\eta})$ which is related to the corresponding free t_{ij} matrix of meson-nucleon interaction (as in eq. (17))

At present our calculations have been carried out only for the first part of eq. (16), the plane wave impulse approximation (*PWIA*). At this level, however, we do not perform any approximation treating the full spin degrees of freedom and taking Fermi motion effects of the nucleon into account by performing the integration in momentum space. For deuteron[16]) and ^{3}He/^{3}H[17]) we use realistic nuclear wave functions. In the case of ^{4}He with $J = T = 0$ a phenomenological nuclear formfactor is used which has been extracted from the charge distribution of ^4He.

In application of eta photoproduction on light nuclei with well-known nuclear structure we can study details of the elementary production operator which are not resolved in the elementary reaction or, as for the neutron amplitude, are not experimentally accessible. In the deuteron case only the isoscalar amplitude contributes; in ^{3}He the two protons saturate to spin 0 and contribute only to a very small part via the non–spin amplitude from $P_{11}(1440)$ and background terms, while the residual neutron gives rise to a strong E_{0+} amplitude. Finally, in the case of ^{4}He we can study the coherent amplitude of $t_{\eta\gamma}$ which is the isoscalar non–spin flip part which arises entirely from small magnetic multipoles, e.g. M_{1-} and M_{1+}.

We start our discussion with the deuteron in Fig. 4. In this case experimental data are available which seems to be in large disagreement with the predictions of *PWIA*. As mentioned earlier, our model and also quark models give rather small isoscalar (γ,η) amplitudes with $E_{0+}^{(0)}/E_{0+}^{(p)} = 0.23$. Only an unrealistically large isoscalar amplitude of $E_{0+}^{(0)}/E_{0+}^{(p)} = 0.8$ can explain the data in *PWIA*. In this case the final state interaction and the coupled $\pi\eta$–channels of eq. (16) may be able to explain the discrepancy. It remains to be seen, however, if the isoscalar amplitude is really as small as in all present models. At this point it is very interesting to note that in the study of π^0 photoproduction on the deuteron a similar puzzle appeared which was finally solved by pion rescattering processes[18]).

In Fig. 5 we show the ratio of eta photoproduction from ^{3}He and ^{3}H and compare this ratio to the ratio of neutron and proton. Over most of the energy range the two curves are close to each other proving that the simple argument also holds in more realistic calculations. Furthermore this curve shows also the sensitivity to the isoscalar amplitude. As in the case of free nucleons, the cross section is not sensitive to the sign of the amplitudes, i.e. the cross section would be the same for a pure isoscalar and a pure isovector amplitude.

Finally in Fig. 6 we show the differential cross sections for all light nuclei up to ^{4}He. Whereas the angular distribution is rather flat for nucleons, as expected from s-wave dominance, it appears more and more peaked in forward direction for $A > 1$. This reflects the signature of the nuclear

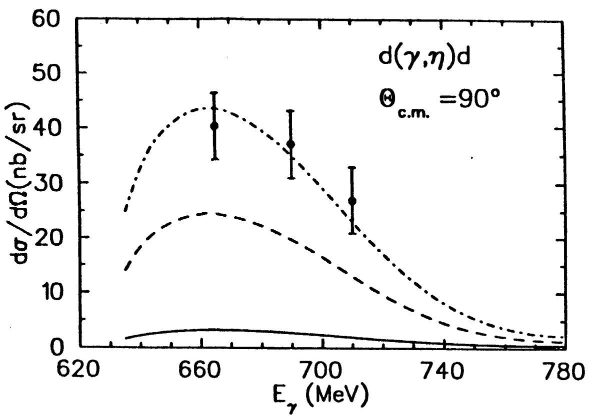

Fig. 4: Differential cross section for eta photoproduction on the deuteron. The solid curve has been obtained with our model described in the text with $E_{0+}^{(0)}/E_{0+}^{(p)} = 0.23$. The dashed and dash–dotted curves are obtained with ratios of 0.6 and 0.8 respectively. The experimental data are from ref. [20]).

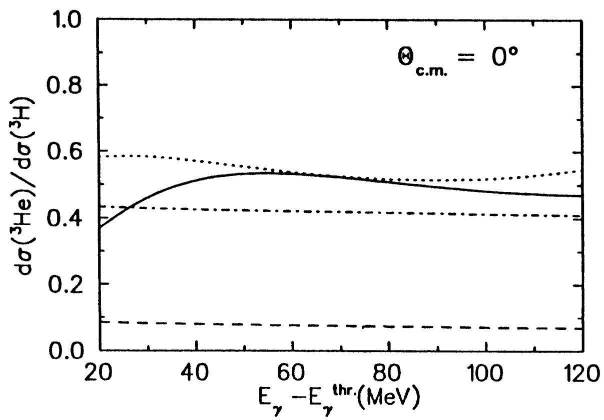

Fig. 5: Ratio of differential cross sections of eta photoproduction on ^{3}He and ^{3}H at forward direction. The dotted line shows the ratio of neutron to proton for comparison. The dashed and dash-dotted curves show the ^{3}He to ^{3}H ratio with $E_{0+}^{(0)}/E_{0+}^{(p)} = 0.6$ and 0.8 respectively.

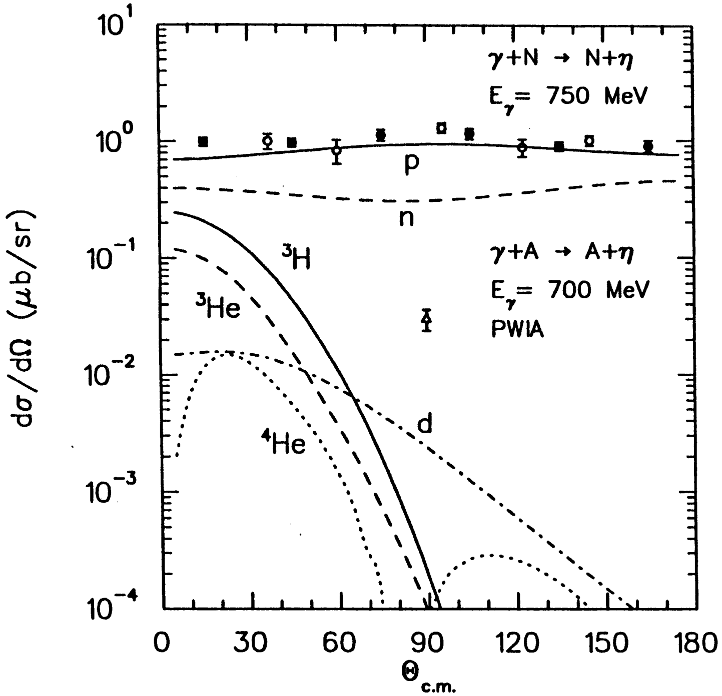

Fig. 6: Differential cross section for eta photoproduction on p, n, d, ^{3}He, ^{3}H and ^{4}He. The experimental data on the proton are from ref. [7] (•) and ref. [4] (o), the data point on the deuteron is from ref. [20] (▵).

formfactors as the momentum transfer in η photoproduction is rather large, $Q^2 = 7.8\ fm^{-2}$ at threshold. The biggest cross section can be expected for the trinucleon; it is proportional to the free nucleon cross section multiplied by the square of the trinucleon formfactor. However around 90° the cross section on the deuteron gains over the trinucleon, in particular due to the not yet understood enhancement seen in the experiment. The coherent cross section for ^4He vanishes for $\Theta = 0$ and reaches roughly the $10nb$ level in a small angular region. For most angles it falls below $1nb$.

4. Summary and Conclusions

We have presented a model for eta photoproduction on the nucleon and have applied it on all light nuclei, d, ^{3}He, ^{3}H and ^{4}He. The model is based on the coupled channels method of Bennhold and Tanabe [11]) with $S_{11}(1535)$, $P_{11}(1440)$ and $D_{13}(1520)$ nucleon resonances. In addition we have added the t-channel vector meson exchange (ω, ρ) and the nucleon Born terms. We have studied the sensitivity of the ηNN coupling and found a preference for pseudoscalar coupling by comparison with existing data on the proton. This situation will soon improve. New measurements have already been performed at Bonn and at Mainz and the data is beeing analysed. However, in order to get information about the isospin nature of nucleon resonances, e.g. the $S_{11}(1535)$, additional experiments on the neutron are needed. This can be realized in eta photoproduction from deuteron and ^{3}He. In the naive quark model the electromagnetic excitation of the S_{11} is almost entirely isovector, in strong disagreement with the available data on the deuteron. Recently Rosenthal, Forest and Gonzales [19]) have shown that a color-hyperfine interaction, responsible also for the E2/M1 ratio of the Δ excitation, can enhance the isoscalar S_{11} excitation considerably.

Acknowledgement

We would like to thank Gisela Anton and Hans Ströher for fruitfull discussions and Rolf Dahm for his help with the REDUCE program.

References

1) D. Drechsel and L. Tiator, J. Phys. G: Nucl. Part. Phys. **18** (1992) 449
2) G. Anton, Contribution to the 7th Amsterdam MINI–conference 1991 and private communication
3) H. Ströher, private communication
4) B. Delcourt et al, Phys. Lett. **B29** (1967) 75
5) C. Bacci et al, Phys. Rev. Lett. **20** (1968) 571; Nuovo Cim. **45** (1966) 983
6) S. Homma et al, J. Phys. Soc. Japan **57** (1988) 828
7) S.A. Dytman et al, Bull. Am. Phys. Soc. **35** (1990) 1679 and Contribution to the Fourth Conf on the Intersection of Particle and Nuclear Physics, Tucson 1991
8) H.R. Hicks et al, Phys. Rev. **D7** (1973) 2614
9) F. Tabakin, S.A. Dytman and A.S. Rosenthal, in Excited Baryons 1988, eds G. Adams, N.C. Mukhopadhyay and P. Stoler, World Scientific 1989
10) M. Benmerrouche and N.C. Mukhopadhyay, Phys. Rev. Lett. **67** (1991) 1070
11) C. Bennhold and H. Tanabe, Nucl. Phys. **A530** (1991) 625
12) R. Brockmann and R. Machleidt, Phys. Rev. **C42** (1990) 1965
13) S.I. Alekhin et al, CERN-HERA 87-01, 1987 (unpublished)
14) S. Kamalov, L. Tiator and C. Bennhold, Few Body Systems **10** (1991) 143
15) A.K. Kerman, H. McManus and R. Thaler, Ann. Phys. (NY) **8** (1959) 551
16) M. Lacombe et al, Phys. Lett. **101B** (1981) 139
17) R.A. Brandenburg, Y.E. Kim and A. Tubis, Phys. Rev. **C12** (1975) 1368
18) J.H. Koch and R.M. Woloshyn, Phys. Rev. **C16** (1977) 1968
19) A.S. Rosenthal, T. Forest and M. Gonzales, Phys. Rev. **C44** (1991) 2765
20) R.L. Anderson and R. Prepost, Phys. Rev. Lett. **23** (1969) 46